Available online at www.sciencedirect.com

ScienceDirect

Procedia CIRP 13 (2014) 264 – 269

www.elsevier.com/locate/procedia

2nd CIRP Conference on Surface Integrity (CSI)

On surface grind hardening induced residual stresses

Konstantinos Salonitis*

Manufacturing and Materials Department, Cranfield University, Cranfield MK43 0AL, UK

* Corresponding author. Tel.: +44 0 1234 758347. *E-mail address*: k.salonitis@cranfield.ac.uk.

Abstract

Grind hardening process utilizes the heat generated in the grinding area for the surface heat treatment of the workpiece. The workpiece surface is heated above the austenitizing temperature by using large values of depth of cut and low workpiece feed speeds. The workpiece undergoes martensitic phase transformation increasing its hardness in the surface layer. Usually compressive residual stresses are induced in the surface layer. In the present paper, modeling and prediction of the residual stresses profile as a function of the process parameters is presented. The model's results are validated for two cases; a dry grind hardening and a coolant assisted grind hardening of AISI 1045 steel.

Selection and peer-review under responsibility of The International Scientific Committee of the "2nd Conference on Surface Integrity" in the person of the Conference Chair Prof Dragos Axinte dragos.axinte@nottingham.ac.uk

Keywords: Residual stresses; Finite element method; grinding; grind-hardening

1. Introduction

Grind-hardening (Figure 1) is a hybrid manufacturing process that can simultaneously harden and grind a workpiece. The process relies on controlling the generated heat for heating locally the processed workpiece in order to increase its surface hardness. The metallurgic change required for the hardening is achieved by heating the surface above austenitization temperature and through the subsequent quenching martensitic transformation is induced on the workpiece surface.

The grind hardening process was introduced by Brinksmeier and Brockhoff [1]. Initially the process was investigated experimentally [2] in order basically to prove its feasibility. Salonitis et al. presented a number of theoretical studies, covering a number of different aspects such as the thermal analysis of the process [3], the cutting fluid significance [4], the grinding wheel specifications effect [5] and recently the grinding forces [6]. However, grind-hardening induced residual stresses simulation has not been presented up to now.

In a number of experimental studies it has been shown that grind-hardening results in compressive residual stresses [1, 7]. Nguyen et al. [8] on the other hand showed experimentally that grind-hardening in dry air results in tensile residual stresses, whereas when using coolant compressive residual stresses are induced.

However, there is no investigation in the literature indicating whether the residual stresses profile can be affected, and potentially optimized, by the main parameters. The main process parameters are the workpiece speed, the depth of cut, the cutting speed, the workpiece material, the grinding wheel type and the presence of a cutting fluid. Most of the published works have concentrated on modeling the effect of these process parameters on Hardness Penetration Depth (HPD), hardness distribution and process induced forces.

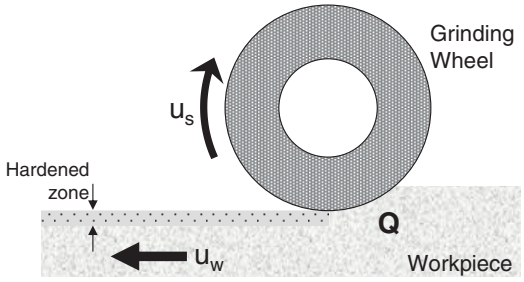

Fig. 1. Grind-hardening process

Selection and peer-review under responsibility of The International Scientific Committee of the "2nd Conference on Surface Integrity" in the person of the Conference Chair Prof Dragos Axinte dragos.axinte@nottingham.ac.uk
doi:10.1016/j.procir.2014.04.045

The scope of the present paper is the development of a finite element model for surface grind hardening process able to predict the residual stresses profile. The validation of the model is conducted by comparison with experimental data.

2. Theoretical Analysis

2.1. Grind hardening process modeling framework

The simulation work that has been published up to now is limited to the determination of the surface hardness and the hardness penetration depth. The usual modeling approach is depicted in figure 2. However for the complete prediction of the grind hardness performance, the residual stresses should be determined as well. As it can be seen in figure 2, a coupled structural FEA model needs to be developed for the estimation of the residual stresses. In the present paper, the focus is in the orange steps indicated in figure 2, however the rest of the steps are briefly discussed for the sake of completeness.

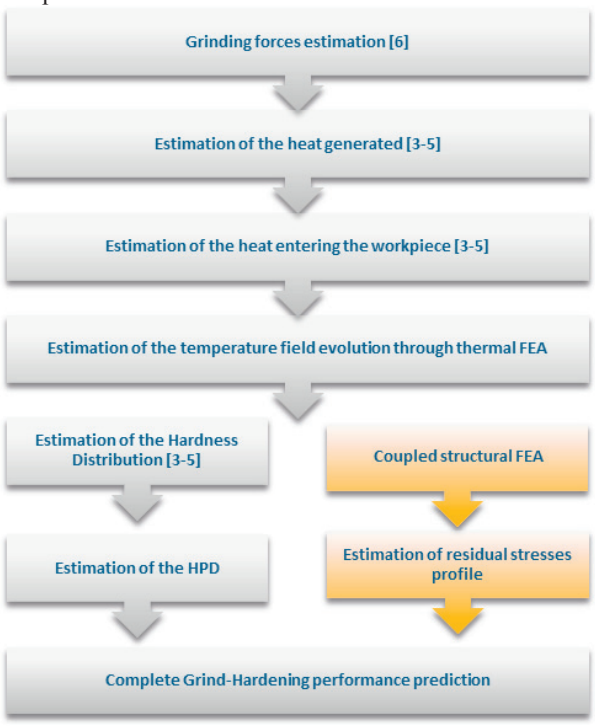

Fig. 2. Grind-hardening modeling approach

2.2. Grind hardening process mechanisms

The grind hardening process is characterized by very complex physical mechanisms that depend on a number of characteristics. As already indicated, there are a number of process parameters that affect the process outcome. The hardening of the surface layer is achieved by raising the surface temperature above that of austenitisation and subsequently, (as the grinding wheel passes over) the rapid cooling (quenching) of the workpiece material through convection to the coolant fluid and through conduction to the rest of the workpiece material. The cooling results in transforming the crystal lattice of the material into martensite that poses the elevated hardness. It is therefore evident that one of the most important issues of the process is that of the heat generation mechanism.

As indicated, the heat generation is the result of the grinding wheel and the interaction of the workpiece material. The heat generation mechanism and the partition of the heat to the grinding wheel, the workpiece, the chips and the coolant fluid has been investigated theoretically in a number of studies [3-5]. The heat generation is attributed to the friction among the abrasive grains and the workpiece material. The heat absorbed by the workpiece can be estimated with the use of the simplified heat partitioning model, developed by Rowe et al. [9].

The actual amount of heat generated during the process equals the grinding wheel spindle power,

$$P = F_t \cdot u_s \tag{1}$$

where P, is the grinding wheel spindle power, F_t is the tangential component of the cutting forces and u_s is the grinding wheel speed. The cutting forces depend on the process parameters, the grinding wheel topography and the workpiece material [6]. It was concluded that the sliding component of the cutting forces account almost for 97% of the total forces. For the present study, the closed form equation derived in study [6] will be used for the estimation of the cutting forces and subsequently, the heat generation rate can be estimated from eq. (1). Alternatively, empirical approaches can be used for estimating the grinding forces [10].

Knowing the heat generation rate, the heat that is absorbed by the workpiece can be estimated. At typical grind-hardening workpiece speeds, the heat partition to the grinding wheel is in the range of 35–55% whereas the heat partition to the workpiece is in the range of 40–60% [4, 11].

Once the heat entering the workpiece has been determined, using FEA, the temperature field can be determined. The micro-hardness of the workpiece material can be determined with the use of the transformed Continuous Cooling Temperature (CCT) diagrams so as to account for the rapid heating of the material [4]. The HPD afterwards, can be calculated from the hardness distribution, as the depth from the workpiece surface, where the hardness value is reduced

to 80% of the nominal value. Alternatively, it can be estimated from the depth, where the temperature exceeds the austenitisation temperature [11]. However, the latter assumption is valid only when the critical quenching has been achieved as indicated in [4].

2.3. Determination of temperature field and HPD

A FEA thermal model is constructed for calculating the temperature field. A simple orthogonal workpiece was considered. Since the heat source width is at least one order of magnitude larger than the heat penetration depth, the workpiece was modeled as a 2-D rectangle with infinite length. Tetrahedral finite elements have been used for the meshing of the geometry. The distribution of elements is denser on the workpiece surface and their size increases gradually while moving away from it (Figure 3.a).

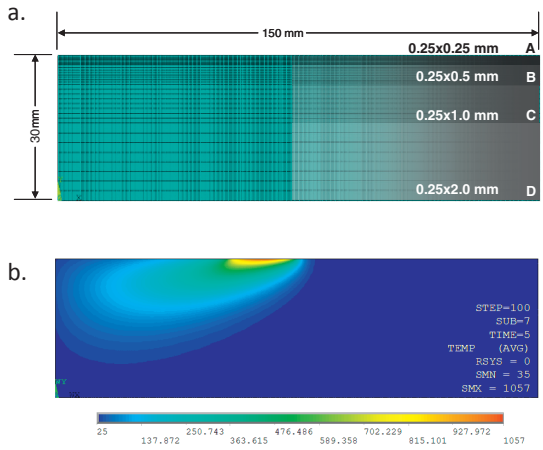

Fig. 3. a. 2-D Finite element model and b. resulting temperature distribution for a specific load step

The heat source was considered having triangular heat distribution. The length of the heat source is equal to the grinding wheel – workpiece geometrical contact length. The heat transfer problem was considered a quasi-stationary one. The boundary conditions include all possible heat transfer mechanisms such as heat radiation, heat convection due to coolant application locally and heat conduction within the workpiece material. The workpiece feed speed was modeled through the movement of the heat source, on the workpiece surface, with a constant velocity equal to that of the workpiece feed. The loading of the model thus is done in load-steps, with the elements corresponding to the position of the heat source (contact between grinding wheel and workpiece) being loaded for a short period of time equal to the contact time. The final cooling of the workpiece to environmental temperature is also considered with additional load-steps, although no additional loading of elements is needed.

The FEA solution provided the temperature profile, induced in the workpiece material during the grind hardening (Figure 3.b). The temperature field as a function of process parameters was calculated from the FE model. In Figure 4, the temperature change over time for various distances from the workpiece surface is shown.

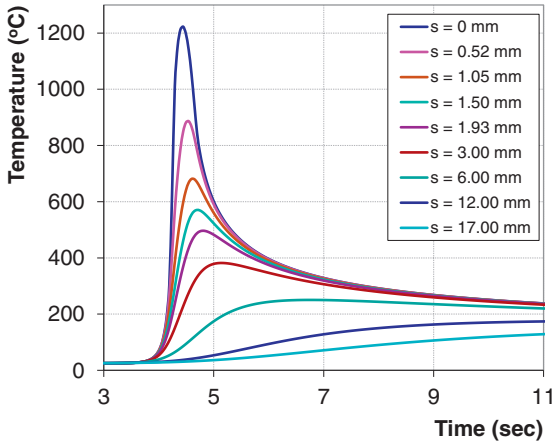

Fig. 4. Temperature change over time as a function of the distance from the workpiece surface (l_c = 11 mm, u_w =0.6 m/min ,a_e=0.3mm)

In figure 5, workpiece temperature as a function of the distance from the workpiece surface is shown for various heat flux values, when grind hardening with workpiece speed equal to 0.6 m/min, depth of cut equal to 0.3 mm and grinding wheel having 400 mm diameter.

HPD can be assumed to be the depth where the temperature reaches austenitisation temperature. Relations between HPD and heat flux, workpiece speed and contact length have been derived and are shown in Figure 6. HPD is considered to be bound by a maximum value, as discussed in [3], that is related to the heat flux that would cause melting on the workpiece surface.

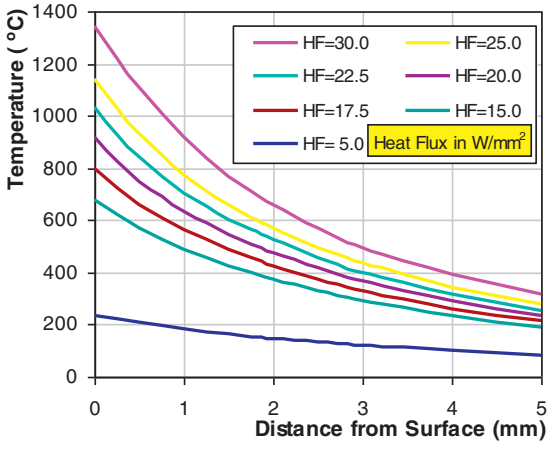

Fig. 5. Maximum temperature as a function of the distance from the workpiece surface (l_c = 11 mm, u_w =0.6 m/min ,a_e=0.3mm)

The continuous lines in Figure 6 have been determined theoretically. Experimental calibration has resulted in the dashed ones [5]. A database composed of such charts was established allowing the determination of the requested heat flux value, in typical grind hardening processes, for a pre-specified HPD.

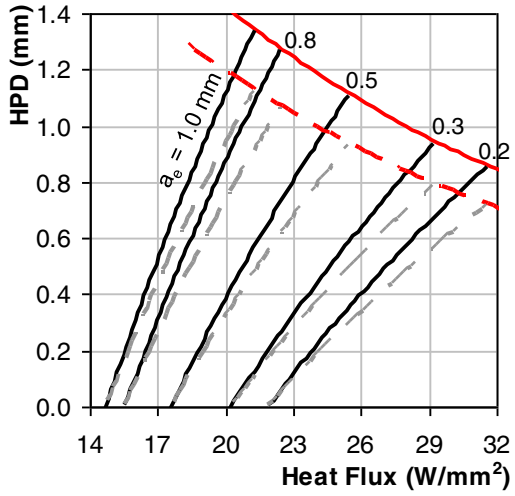

Fig. 6. HPD, Heat flux and process parameters correlation

2.4. Determination of residual stresses

Surface residual stresses on ground workpieces is a result of the thermal deformation due to heat dissipation in the grinding zone, the pressure between the grinding wheel and the workpiece, and the phase transformation of the material structure [12]. The balance between these three different mechanisms defines whether the final residual stresses are compressive or residual. It has been shown in past studies, focusing though on grinding and not grind-hardening, that the pressure applied from the grinding wheel to the workpiece induces compressive residual stresses. On the other hand thermal deformation due to the heat dissipation results in tensile residual stresses [13]. The challenge is to incorporate the resulting residual stresses due to phase transformation. Phase change results in volume change; depending on whether the new structure occupies more space than the original phase the residual stresses can be either compressive or tensile. For the case of grind hardening we observe two subsequent phase transformations. From ferrite/perlite mixture before grinding to austenite (existing only when the workpiece material is above eutoctoid temperature) during the processing and finally to martensite due to quenching. Martensite presents body-centred tetragonal (BCT) crystal structure whereas ferrite presents body-centred cubic (BCC) crystal structure [14]. Since BCT occupies more space than BCC, martensitic phase transformation results into compressive residual stresses.

In the present paper, the residual stresses are determined using a FEA model. The thermal model developed in section 2.3 is used as a basis. Thermal elements are replaced with elastic-plastic elements. The resulting model undergoes an elastic-plastic structural analysis using temperature-dependent material properties and a multi-linear isotropic hardening model is used.

For each load step, the nodal temperatures from the thermal analysis are read into the structural analysis. Nodal temperatures from thermal results are continued to be read into the structural analysis until the time when the model temperature has reached the environmental one. The structural boundary conditions set to workpiece are quite simple; all nodes at the bottom end of the workpiece are fixed to all directions. The structural loading includes the application of pressure resulting from the grinding wheel – workpiece interaction at the elements that corresponds to the contact length for each load-step.

The FEA analysis results in the residual stresses due to the grinding arc pressure (mechanical) and the thermal deformation. The residual stresses due to phase transformation cannot be determined directly. For this reason a module is developed that calculates for each node the resulting stress due to phase change. The phase change is determined by the continuous cooling temperature (CCT) diagram with input the temperature cycle (provided by the thermal FEA). The final total residual stresses are calculated through superposition of the stresses values.

The model approach can be illustrated as a flow chart (figure 7).

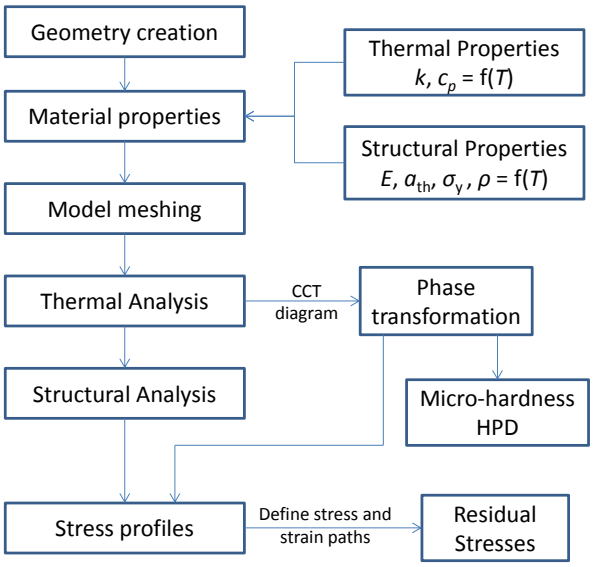

Fig. 7. FEA modeling approach

3. Theoretical Model Validation

The model's predictions were validated using experimental results. Surface grinding experiments were conducted on an annealed AISI 1050 material with a depth of cut of 0.30 mm, feed speed of 0.4 m/min and a wheel speed of 26 m/s. Two different experiments were conducted, one under dry conditions and one with an oil based coolant applied with a flow rate of 15.0 L/min. The micro-hardness measured on the basic material was 190±15 $HV_{0.5}$.

3.1. HPD prediction validation

The main reason for using grind-hardening is to increase the surface hardness of the workpiece to a specific depth. The hardness penetration depth (HPD) is the metric for assessing the process performance. As it has been pointed out in [4], HPD can be determined either from the calculated hardness distribution or from the depth, where the temperature exceeds the austenitisation temperature. Latter method is used in the present paper for ease of calculation. Experimentally, the HPD can be determined from the measured micro-hardness. In figure 8, the experimental and theoretical HPD is compared for both cases.

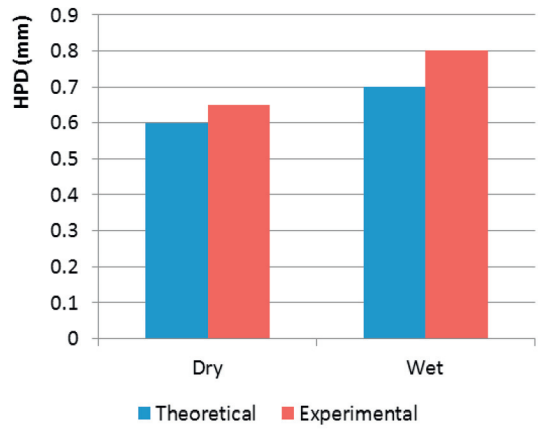

Fig. 8. HPD comparison for dry and wet grind-hardening process

Obviously, the utilization of coolant fluid decreases the surface temperature. The application of coolant fluid increases the cooling rate, affecting significantly the heat treatment cycle, changing the critical temperature that crystal structure changes phase. Additionally the surface temperature reduction results in higher surface hardness values since less austenite is retained after the completion of the process [4].

The surface hardness achieved using both approaches were the same with an average value of 740 HV, which is 3.9 times higher that of the basic material. The micro-hardness till HPD was constant. This is due to the fact that the maximum hardness value that can be expected is a function of the chemical composition of the material.

3.2. Residual stresses prediction validation

The residual stresses on the ground workpiece was estimated using the FEA model for both cases. The distribution of residual stresses are shown in Fig. 9 and 10 for dry and wet conditions respectively. In both figures, σ_{xx} and σ_{yy} are residual stresses calculated along and perpendicular to the grinding direction, respectively.

Additionally, the residual stresses were measured experimentally with an X-ray diffraction apparatus (Rigaku).

Grind-hardening without the application of coolant fluid resulted in tensile residual stresses across the whole depth of the heat treated layer in both directions. Simulation presents the same result with a mediocre accuracy of 20%. Using the FEA model, it was shown that during dry grind-hardening the driving mechanism for the resulting residual stresses is the thermal deformation due to the high heat source generated in the grinding arc. Additionally, higher workpiece material results in lower martensite onset temperatures, that leads to higher concentration of retained austenite. Austenite presents face-centered cubic (FCC) lattice structure with quite similar volume with original ferrite (BCC), thus the compressive stresses due to phase transformation are limited.

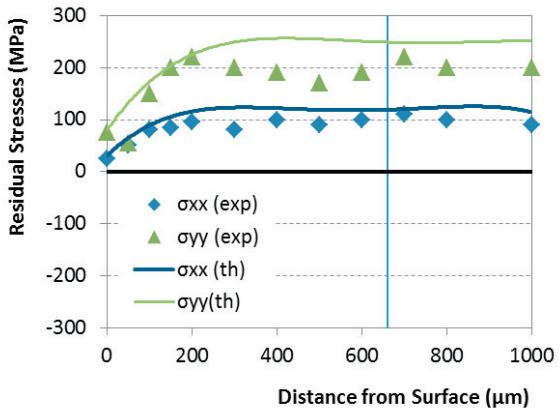

Fig. 9. Residual Stresses after dry grind-hardening at the middle of the workpiece (Vertical line indicated the length of hardened layer)

Assisting the grind-hardening quenching with coolant fluid produces compressive residual stresses up to one fourth the hardened layer for both measured directions. The use of coolant fluid increases the efficiency of martensite transformation. Additionally, the surface temperature is reduced (from almost 1200°C to 900°C according to FEA results), reducing the thermal

deformation of the workpiece that results into tensile stresses. The FEA calculated residual stresses present similar trends.

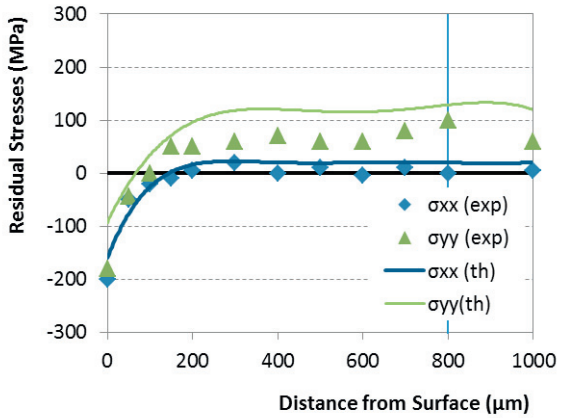

Fig. 10. Residual Stresses after wet grind-hardening at the middle of the workpiece (Vertical line indicated the length of hardened layer)

4. Conclusions

The present study has been focused on the grind-hardening induced residual stresses. In general, compressive stresses are welcome for engineering applications, as tensile surface residual stresses facilitate fracture, fatigue failure, corrosion and wear.

A FEA model has been developed for the estimation of the residual stresses and the hardness penetration depth. Experimental results have verified the theoretical predictions. FEA results present similar trends with regards the residual stresses. The accuracy of the FEA model is adequate, however further work is needed for tuning the model.

References

[1] Brinksmeier, E., Brockhoff, T., 1996. Utilization of Grinding Heat as a New Heat Treatment Process. Annals of the CIRP 45/1, pp. 283–286.

[2] Brockhoff, T., 1999. Grind-hardening: A comprehensive View. Annals of the CIRP 48/1, pp. 255 – 260.

[3] Salonitis, K., Chryssolouris, G., 2007, Thermal analysis of Grind-Hardening process. International Journal of Manufacturing Technology and Management 12, pp. 72-92.

[4] Salonitis, K., Chryssolouris, G., 2007. Cooling application in Grind-Hardening Operations. International Journal of Advanced Manufacturing Technology 33, pp. 285-297.

[5] Salonitis, K., Chrondros, T., Chryssolouris, G., 2008. Grinding wheel effect on grind-hardening process. International Journal of Advanced Manufacturing Technology 38, pp. 48-58.

[6] Salonitis, K., Stavropoulos, P., Kolios, A., 2014. External grind-hardening forces modelling and experimentation. International Journal of Advanced Manufacturing Technology 70, pp. 523-530,

[7] Kolkwitz, B., Foeckerer, T., Heinzel, C., Zaeh, M.F., Brinksmeier, E., 2001. Experimental and Numerical Analysis of the Surface Integrity resulting from Outer-Diameter Grind-Hardening. Procedia Engineering 19 (2011) 222 – 227

[8] Nguyen, T., Zarudi, I., Zhang, L.C. (2007). Grinding-hardening with liquid nitrogen: Mechanisms and technology, International Journal of Machine Tools & Manufacture 47, pp. 97–106

[9] Rowe, W.B., Morgan, M.N. Black, S.C.E., 1998, Validation of thermal properties in grinding, Annals of the CIRP, 47/1:275-279.

[10] Mishra, V.K., Salonitis, K., 2013. Empirical Estimation of Grinding Specific Forces and Energy Based on a Modified Werner Grinding Model, Procedia CIRP 8, pp. 287-292.

[11] Chryssolouris, G., Tsirbas, K., Salonitis, K., 2005. An analytical, numerical and experimental approach to grind hardening. Journal of Manufacturing Processes 7/1, pp. 1-9.

[12] Mahdi, M., Zhang, L., 1999. Applied Mechanics in Grinding. Part 7: residual stresses induced by the full coupling of mechanical deformation, thermal deformation and phase transformation. International Journal of Machine Tools and Manufacturing 39, pp. 1285 – 1298.

[13] Mahdi, M., Zhang, L.C., 1997. Applied mechanics in grinding-V. Thermal residual stresses. International Journal of Machine Tools & Manufacture 37, pp. 619–633

[14] Krauss, G., 1993. Steels: Heat Treatment and Processing Principles, ASM International.